Neuroscience 134 (2005) 1179–1194

CILIARY NEUROTROPHIC FACTOR-IMMUNOREACTIVITY IN OLFACTORY SENSORY NEURONS

T. LANGENHAN,[a] M. SENDTNER,[b] B. HOLTMANN,[b] P. CARROLL[c] AND E. ASAN[a]*

[a]*Institute of Anatomy and Cell Biology, University of Wuerzburg, Koellikerstr. 6, 97070 Wuerzburg, Germany*

[b]*Institute for Clinical Neurobiology, University of Wuerzburg, Josef-Schneider-Str. 11, 97080 Wuerzburg, Germany*

[c]*INSERM U 583, INM, Institut des Neurosciences de Montpellier, Hopital St. Eloi, 80 rue Augustin Fliche, BP 74103,34091 Montpellier Cedex 5, France*

Abstract—Ciliary neurotrophic factor (CNTF) has been implicated in processes of neuroprotection, axonal regeneration and synaptogenesis in the lesioned CNS. In the olfactory system, which is characterized by particularly robust neuroplasticity throughout life, the concentration of CNTF is high even under physiological conditions. In the present study, the cellular localization of CNTF-immunoreactivity was studied in the rat and mouse olfactory epithelium. In both species, individual olfactory sensory neurons (ONs) displayed intense CNTF-immunoreactivity. The number of CNTF-ir ONs varied interindividually in rats and was lower in mice than in rats. In olfactory epithelia of mice expressing β-galactosidase under control of the CNTF promoter, cells of the ON layer were immunoreactive for the reporter protein. CNTF-ir ONs were olfactory marker protein-positive and growth associated protein 43-negative. CNTF-ir ONs lacked apoptotic markers, and the number of specifically labeled ONs was apparently unchanged after light chemical lesioning of the epithelium, indicating that CNTF-immunoreactivity was not associated with ON death. Electron microscopy of CNTF-ir ON axons in innervated olfactory bulb glomeruli documented that they formed typical ON axonal synapses with target neurons. Three dimensional reconstructions of bulb pairs showed a striking similarity of the positions of glomeruli innervated by CNTF-ir ON axons in left and right bulbs of individual animals and interindividually. The number of innervated glomeruli differed interindividually in rats and was lower in mice than in rats. The results show that in rodents CNTF-immunoreactivity occurs in a subset of mature, functionally competent ONs. The localization of target glomeruli suggests that CNTF-immunoreactivity may be associated with the expression and/or activation of specific olfactory receptor proteins. © 2005 Published by Elsevier Ltd on behalf of IBRO.

Key words: olfactory epithelium, neuronal cell death, olfactory information processing, electron microscopy.

Olfactory sensory neurons (ONs) are the only neurons situated in a surface epithelium, and resemble other epithelial cells in that they form typical intercellular junctions with cells surrounding them, creating an epithelial barrier (Miragall et al., 1988; Asan and Meier-Stiegen, 1998). Despite these unusual properties, ONs are true neurons. The single axons of individual ONs run directly into the telencephalon, and terminate in one particular glomerulus of the ipsilateral olfactory bulb (OB). Each ON expresses only one of a large family (~1000 members in mice) of odorant receptor proteins (OR). Individual ORs possess high affinity for specific molecular features of odorants, and thus endow the subpopulation of ONs which synthesize them with characteristic odorant response sensitivities. All ONs expressing the same OR project to a limited number of bilaterally symmetrically localized OB glomeruli (Mombaerts et al., 1996), where they form conventional synapses with bulbar projection and interneurons. The topographical arrangement of glomeruli activated by specific odorants represents an olfactory sensory map which appears to be fundamental for olfactory information processing (Schwob, 2002; for reviews see Nagao et al., 2002).

Since they are directly exposed to the environment, ONs are vulnerable, and massive ON death can be caused by toxic or infectious agents in the air (e.g. Cowan and Roskams, 2002). An acute or gradual loss of the sense of smell, which would be life-threatening at least in macrosmatic animals, is prevented by continuous ON neurogenesis from neuronal precursors situated in the olfactory epithelium (OE; e.g. Mackay-Sim and Chuah, 2000; Schwob, 2002; Nibu, 2002). Newly formed neurons have to regrow their axons into the predestined glomeruli, and to form synapses with target neurons in the OB (Schwob, 2002). Thus, neurogenesis, targeted axogenesis and synaptogenesis are permanently occurring in the peripheral olfactory system. Additionally, olfactory learning processes afford continuous plasticity of existing synapses in the OB (Matsuoka et al., 1997). In rodents and primates, moreover, interneurons of the OB are continuously generated in the forebrain subventricular zone, migrate along the "rostral migratory stream" into the OB, and are integrated into preexisting neuronal circuits (e.g. Gheusi et al., 2000).

Neurotrophic factors are known to be essential for neuroplasticity in the nervous system both during embryonic development and in the adult and have been shown to be expressed in the peripheral olfactory system at high levels throughout life (Schwob et al., 1992; Mackay-Sim

*Corresponding author. Tel: +49-931-312715; fax: +49-931-312712.

Abbreviations: a-CNTFm, monoclonal mouse-anti-rat ciliary neurotrophic factor; BL, basal cell layer; CASP, activated caspase 3; cha-CNTFp, polyclonal chicken-anti-ciliary neurotrophic factor; CNTF, ciliary neurotrophic factor; DAB, 3,3′-diaminobenzidine; DAPI, 4′,6-diamidin-2′-phenylindol-dihydrochlorid; GA, glutaraldehyde; ga-CNTFp, polyclonal goat-anti-ciliary neurotrophic factor; GAP43, growth-associated protein of 43 kD; GOD, glucose oxidase; -ir, -immunoreactive; NDS, normal donkey serum; NGS, normal goat serum; NiDAB, nickel-intensified 3,3′-diaminobenzidine; OB, olfactory bulb; OE, olfactory epithelium; OL, olfactory sensory neuron layer; OMP, olfactory marker protein; ON, olfactory sensory neuron; OR, odorant receptor protein; PBS, phosphate-buffered saline; PFA, paraformaldehyde; ra-CNTFp, polyclonal rabbit-anti-rat ciliary neurotrophic factor; RT, room temperature.

0306-4522/05$30.00+0.00 © 2005 Published by Elsevier Ltd on behalf of IBRO.
doi:10.1016/j.neuroscience.2005.05.017

and Chuah, 2000; Cowan and Roskams, 2002; Miwa et al., 2002). Ciliary neurotrophic factor (CNTF), a member of the four alpha-helical cytokine family including interleukin 6, leukemia inhibitory factor, and others (Sendtner et al., 1994; Weisenhorn et al., 1999) has gained increasing attention in recent years due to its possible actions in physiological maintenance and injury response of the adult nervous system (Weisenhorn et al., 1999). Additionally, approximately 3% of the human population are CNTF-deficient (Takahashi et al., 1994; Thome et al., 1997), and recent reports indicate an involvement of the CNTF-deficiency in neurological disease (Giess et al., 1998; Linker et al., 2002). Elucidation of the role of CNTF in plasticity of the nervous system may be of considerable importance not only for therapeutic strategies, but also for resolving the etiology of neuropsychiatric diseases. CNTF synthesis is restricted to the postnatal nervous system (Stöckli et al., 1991). The factor has been localized primarily in glial cell types, with highest concentrations in Schwann cells, and in white matter tract astrocytes of the CNS (Dallner et al., 2002). In CNS gray matter astrocytes, it is upregulated after lesions or in deafferented areas (e.g. Guthrie et al., 1997; Lee et al., 1997a). Based on these findings, it has been suggested that CNTF may play a role not only for the survival of injured neurons, but also for maintenance and/or regeneration of neuronal processes and contacts (Stöckli et al., 1991; Winter et al., 1995; Lee et al., 1997a; Dallner et al., 2002). In our recent study on CNTF in the rat and mouse OB, we confirmed that CNTF is localized in ensheathing cells of the olfactory nerve (Asan et al., 2003; Lipson et al., 2003), possibly contributing to the axon-growth promoting properties of these cells (e.g. Smale et al., 1996; Perez-Bouza et al., 1998; Tisay and Key, 1999; Mackay-Sim and Chuah, 2000; Barnett et al., 2000; Bartolomei and Greer, 2000; Raisman, 2000; Lipson et al., 2003). Additionally, we observed scattered intensely CNTF-immunoreactive (-ir) fibers in the olfactory nerve layer which coursed into and ramified in individual olfactory glomeruli, and which we identified as ON axons by colocalization studies (Asan et al., 2003). In order to gain information about possible functions of CNTF in this unusual neuronal localization, the present study was designed to investigate CNTF-immunoreactivity in the OE and to identify and characterize the neurons from which CNTF-ir axons in the OB originate.

EXPERIMENTAL PROCEDURES

Animals

Rats. Adult male and female Wistar rats were bred in our animal facility or purchased from Charles River (Sulzfeld, Germany).

Wildtype (CNTF+/+), CNTF-Gene knockout (CNTF−/−) and CNTF-lacZ knockin mice. CNTF−/− and CNTF-lacZ knockin mice, in which the nuclear localization signal (NLS) from the small T antigen (Kalderon et al., 1984) and the coding sequence for bacterial β-galactosidase had been introduced into the CNTF locus (Masu et al., 1993; Asan et al., 2003), were continuously bred under essentially germ-free conditions in the animal facility of the Neurology Clinics, Würzburg, and backcrossed to C57Bl/6 mice supplied from Charles River at least every third generation. Heterozygous mice were genotyped by Southern blot analysis as described (Masu et al., 1993) and intercrossed to produce F1 offspring which contained both mice with CNTF−/−, CNTF-lacZ knockin and CNTF +/+ genotype. These mice were either directly used or further propagated for one generation for production of animals used in this study. The mice were routinely screened for viral infections and were essentially free of infections with mouse hepatitis virus, reovirus type 3, Theiler's encephalomyelitis virus, pneumonia virus of mice, Sendai virus, and minute virus of mice.

For investigations into the effect of lesions of the OE, adult male CNTF+/+ and −/− mice were instilled with 20–50 μl of 0.7% Triton X-100 in physiological saline into the right nostril under light ether anesthesia (Oberto et al., 2001; e.g. Schwob, 2002). They were subjected to perfusion fixation as described below 0.5 h (n=3 CNTF +/+, n=2 CNTF −/− mice), 1 h (n=2 CNTF +/+, n=1 CNTF−/− mice) and 24 h (n=1 CNTF +/+) post-lesionem. One CNTF +/+ mouse and one CNTF −/− mouse were instilled with saline alone and perfused after 24 and 0.5 h, respectively.

All animal experiments were done conforming to the guidelines on the ethical use of animals according to the German Law for the Protection of Animals, and were designed to minimize the number of animals used and their suffering.

Immunocytochemistry

Tissue preparation: Fixed tissue. Rats (n=20) were anesthetized and, after a short pre-rinse, perfused transcardially with either 4% paraformaldehyde (PFA) in 0.01 M phosphate-buffered saline for 15 min (PBS; Fixative I); 4% PFA in 0.2% sodium acetate pH 6.5 for 10 min followed by 20 min 4% PFA in 0.1 M sodium carbonate–bicarbonate at pH 11 containing 0.2% glutaraldehyde (GA; Fixative II; Berod et al., 1981; Liposits et al., 1986); or 4% PFA and 15% saturated picric acid in 0.1 M phosphate buffer (PB) pH 7.2 containing 0.08% GA for 10 min (Fix III). Adult mice of both sexes (wildtype: n=25, seven animals post-lesionem as described above; CNTF−/−: n=8; four animals post-lesionem; homozygous and heterozygous CNTF-lacZ knockin mice: n=2 each) were perfused using Fix I for 10 min. After perfusion, olfactory tissue (epithelium and bulb) was dissected. To facilitate sectioning of OE, as much bone as possible was separated from the block of nose containing turbinates and septal tissue. In two rats, septal and lateral nose walls including turbinates were dissected as whole mounts. Dissected tissue was postfixed for 3 h at room temperature (RT) or overnight at 4 °C. Tissue for light and fluorescence microscopy was washed in PBS, and whole-mount preparations were directly processed for immunohistochemistry as described below. The other preparations were infiltrated successively with 10% and 20% sucrose in PBS, submerged in a drop of Tissue Freezing Medium (Leica Instruments, Nussloch, Germany) on cork supports, frozen in liquid nitrogen-cooled isopentane, and stored at −80 °C. Sections were cut either using a cryostat (10–30 μm) or, after gradual thawing to RT, using a vibratome (30–50 μm; Leica VS, Leica Instruments, Bensheim, Germany). Nose tissue from five rats was decalcified by immersion in 5% EDTA in 0.1 M Soerensen buffer for 6 days with daily buffer changes. Decalcified tissue was paraffin-embedded and cut on a sliding microtome at 5 μm. From OBs of five wildtype mice, three male and three female rats and from nose tissue of all lesioned mice, series of cryostat sections were prepared (six series of 16 or 20 μm sections for OBs of mice and rats, respectively, and four series of 12 μm sections for nose tissue). One of the series was stained for cytoarchitectonic details using gallocyanin-staining (OBs; Heinsen et al., 2000) or hematoxylin-eosin staining (OE). The other series were used for immunoreactions (see below).

Tissue for electron microscopy was washed in PBS after postfixation and immediately vibratome sectioned. Vibratome sec-

tions were either directly processed for immunocytochemistry or stored in cryoprotective solution at −40° until needed.

Native tissue for TUNEL labeling, β-galactosidase histochemistry or freeze-drying. Rats ($n=5$) or mice (CNTF wildtype: $n=2$, CNTF-lacZ knockin homo- and heterozygous, $n=1$ each) were decapitated in ether anesthesia and nose tissue was dissected. For cryosectioning, blocks of ca. 5 mm^3 were covered with Tissue Freezing Medium on pieces of cork and frozen in liquid-nitrogen-cooled isopentane. For freeze-drying, smaller blocks (ca. 1 mm^3) were rapidly frozen in liquid-nitrogen-cooled isopentane. Freeze-drying, Epon embedding, semithin sectioning and etching of sections were performed according to established protocols (Drenckhahn and Franz, 1986).

Antibodies. Four different CNTF-antibodies were used for the experiments: polyclonal rabbit-anti-rat CNTF (ra-CNTFp; IgG fraction; Masu et al., 1993; dilution 1:500–1:5000), monoclonal mouse-anti-rat CNTF (a-CNTFm; 1:250–1:1000), polyclonal goat-anti-CNTF (ga-CNTFp; R&D, Wiesbaden, Germany; 1:500) and polyclonal chicken-anti-CNTF (cha-CNTFp; Promega, Mannheim, Germany, 1:100). All antibodies were generated against recombinant rat CNTF. Goat-anti-olfactory marker protein (OMP)-antiserum was a gift of Dr. F. Margolis, Baltimore, USA. Other antisera and antibodies used were: polyclonal rabbit-anti-β-galactosidase (Sigma, Deisenhofen, Germany, 1:200), monoclonal mouse-anti-growth-associated protein 43 (GAP43; Boehringer, Mannheim, Germany, 1:50–1:100), and polyclonal rabbit-anti-cleaved caspase-3 (CASP)-antibody (Cell Signaling Technology, New England Biolabs, Frankfurt, Germany, 1:500). Lower dilutions were used for immunocytochemistry on mounted cryostat or semithin sections, higher dilutions for reactions using free-floating cryostat and vibratome sections. Secondary antisera for immunoenzyme histochemistry were biotinylated goat-anti-mouse, goat-anti-rabbit or rabbit-anti-goat IgG (Vector, Burlingame, CA, USA or Rockland, Gilbertsville, PA, USA or Dako, Hamburg, Germany; dilution 1:300–500). Secondary antisera for immunofluorescence were Cy2- or Cy3-labeled goat-anti-rabbit, goat-anti-mouse IgG, goat anti-chicken IgY, donkey-anti-rabbit and donkey-anti-goat IgG (Dianova, Hamburg, Germany, Amersham, Freiburg, Germany; Abcam, Cambridge, UK; dilution 1:600).

Immunoreactions for light and fluorescence microscopy. Cryostat sections were thawed onto Superfrost™ slides (Menzel, Braunschweig, Germany) and dried under a cold stream of air for at least 3 h. Paraffin sections were deparaffinized. All sections were then washed in PBS, preincubated in PBS with 2% normal goat serum (NGS), normal donkey serum (NDS; both Sigma) or 0.25% λ-carrageenan (for incubations with primary antibodies generated in goat; Sigma) and 1% Triton X-100 for 1–2 h, and subsequently incubated in the appropriate dilution of the primary antibody (single labeling) or combination of antibodies (double labeling) in 1% NGS or 1% NDS or 0.25% λ-carrageenan, 0.5% Triton X-100 in PBS (incubation buffer) containing 0.05% NaN_3 overnight at 4 °C in a humid chamber. After washing in PBS, sections for single labeling immunoenzyme histochemistry were incubated in the appropriate biotinylated secondary antibody in incubation buffer overnight at 4 °C, washed in PBS, and incubated with StrABC (streptavidin-biotinylated peroxidase complex; Dako) in PBS for 2–3 h. After brief washing in PBS, antigen localization was visualized using the diaminobenzidine–glucose–oxidase method with or without nickel intensification as described (Zaborszky and Heimer, 1989; nickel-intensified 3,3′-diaminobenzidine (NiDAB)–glucose oxidase (GOD)- or 3,3′-diaminobenzidine (DAB)–GOD-method; Asan and Meier-Stiegen, 1998). Sections for single or double labeling immunofluorescence were incubated in the appropriate secondary antibodies in incubation buffer for 3 h at RT or overnight at 4 °C, washed, mounted in 60% glycerol/PBS containing 1.5% *n*-propylgallate (Serva, Heidelberg, Germany) as antifadant, and observed in an Olympus BHS microscope or in a Zeiss LSM 5 confocal microscope. Some cryostat sections were counterstained with DAPI (4′,6-diamidin-2′-phenylindol-dihydrochlorid; Roche, Mannheim, Germany, 1:1000) during the secondary antibody incubation.

Thicker free-floating cryostat sections (40 μm) and vibratome sections were incubated according to the protocol detailed for the cryostat sections, with some modifications: 3 h preincubation, incubation in primary antibodies for 48–72 h at 4 °C, incubation in secondary antibodies overnight at 4 °C. Antigen detection was as described above. Finally, sections were mounted on Superfrost™ slides. For immunofluorescence observation, sections were immediately coverslipped. For immunoenzyme histochemistry, sections were dried, dehydrated, cleared in xylene and coverslipped in DePex.

For detection of CNTF in semithin sections of freeze-dried, Epon-embedded rat OE, the sections were etched as described (Drenckhahn and Franz, 1986), and incubated with the polyclonal rabbit-anti-CNTF-antibody diluted 1:500 in PBS overnight at 4 °C. Washing, secondary antibody incubation and mounting were as described above.

Immunoreactions for electron microscopy. Vibratome sections from rat OB fixed with Fix II and Fix III were treated as described above with minor modifications: preincubation and incubation buffers contained none or 0.04% Triton X-100, respectively. After detection of the antigen with the NiDAB–GOD-method, sections were washed in PBS, osmicated in 1% OsO_4 in PBS for 1 h, washed again in PBS, dehydrated in graded ethanol and finally flat embedded in Epon between sheets of Aclar foil (Plano, Wetzlar, Germany). After polymerization, sections were observed under the light microscope, photographed, and areas of interest were cut out and reembedded onto empty Epon blocks. Ultrathin sections were prepared, floated on formvar-coated grids, contrasted with uranyl acetate and lead citrate (Reynolds, 1963) and observed in a LEO 912 AB (Leo Elektronenmikroskopie, Oberkochen, Germany).

Controls for immunohistochemistry. For the rabbit and monoclonal mouse-anti-CNTF-antibodies, preadsorption controls were carried out. The antibody solutions were incubated overnight at 4 °C with gentle agitation with an excess of recombinant rat CNTF (Asan et al., 2003). After centrifugation, the supernatant was used for immunoenzyme histochemistry as described above on rat tissue in parallel to immunoreactions with the non-preadsorbed antiserum. Specificity was further checked for all antibodies used in every experiment by omitting the primary antibodies from the reaction sequence on some sections, and for mouse tissue by comparison with sections from CNTF−/− mice processed in parallel. In the following descriptions only those structures are presented as immunolabeled for CNTF which, in the rat, could be detected in immunoreactions using all four antibodies (unless specifically mentioned) and which were negative in immunoreactions using preadsorbed antisera. In mice, only those cells were considered specifically labeled that showed reactivity with different antisera and/or which were not labeled in CNTF−/− mice. Immunolabeling and controls for CNTF-immunoreactions in the OB of rats and mice have been described before (Asan et al., 2003).

TUNEL labeling. Cryostat sections were prepared of rat OE fixed with Fix I as described above or of native tissue cryostat sections (12 μm) fixed for 20 min in 4% PFA in PBS at RT. Reactions were carried out using an *in situ* cell death detection kit and a peroxidase-based detection system (Boehringer) according to the manufacturer's description. TUNEL labeling was observed by fluorescence microscopically after fluorescein-labeling of strand breaks and/or after peroxidase detection using the NiDAB–GOD-method. Some sections were additionally immunoreacted

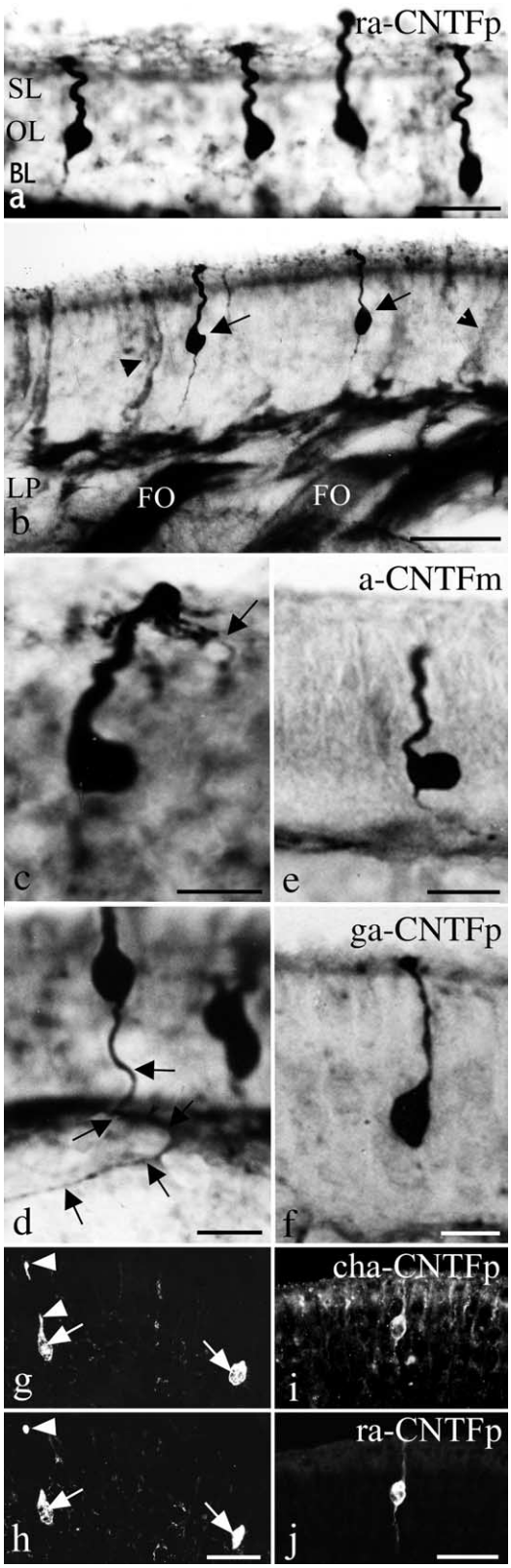

Fig. 1. CNTF-immunoreactivity in vibratome (a–e), cryostat (f, i, j), and semithin sections (g, h) of the rat OE using a polyclonal rabbit antiserum (ra-CNTFp; a–d, g, h, j), a monoclonal mouse antibody (a-CNTFm; e), a polyclonal goat antiserum (ga-CNTFp; f), and a polyclonal chicken antiserum (cha-CNTFp; i). (a) CNTF-ir ONs are localized individually or in groups, with their cell bodies in different sublayers of the OL. (b) In addition to ONs (arrows), cells lining excretory ducts of Bowman's glands (arrowheads) are lightly CNTF-ir. Intense immunoreactivity is found in fila olfactoria (FO). LP, lamina propria; SL, supporting cell layer. (c) Olfactory cilia (arrow) display CNTF-immunoreactivity. (d) CNTF-ir axons (arrows) are observed running through the basal lamina and into the lamina propria. (e, f) Immunoreactive ONs are also detectable using a-CNTFm and ga-CNTFp. (g, h) In serial semithin sections of Epon-embedded, freeze-dried material, CNTF-immunoreaction product fills cell bodies and dendrites (arrowheads) and is also localized in the nuclei (arrows). (i, j) Double labeling using ra-CNTFp and cha-CNTF shows colocalization of immunoreactivities in an ON (arrows) with higher background and lower specific labeling using the chicken antiserum. Scale bars=20 μm in a; b: 30 μm; c–f: 10 μm; in h for g, h and in i for i, j: 20 μm.

for CNTF using polyclonal rabbit-anti-CNTF either directly after strand break labeling followed by detection of CNTF using Cy3-labeled secondary antibodies, or after the TUNEL reaction followed by immunoenzymatic detection using the DAB–GOD-method as described (Liposits et al., 1986; Zaborszky and Heimer, 1989).

Beta-galactosidase histochemistry. Nine micrometer-thick cryosections of OE were cut, freeze-dried, mounted on albuminized slides with celloidin solution and air dried using established methods (Kugler et al., 1985). The mounted sections were reacted with PBS containing 1 mg/ml 5-bromo-4-chloro-3-indolyl-β-D-galactoside (X-gal), 5 mM potassium ferricyanide and potassium ferrocyanide each, 2 mM $MgCl_2$, 0.02% Nonidet-P40 and 0.01% sodium deoxycholate at 37 °C in the dark. To control for unspecific reactions, tissue from CNTF-lacZ knockin and from CNTF wild-type mice was reacted in parallel.

Mapping of glomeruli innervated by CNTF-ir fibers

Gallocyanin-stained series of cryosections from both bulbs (every sixth section of 20 μm thickness in rats and of 16 μm thickness in mice) of one paradigm case each of male rats, female rats and female mice were photographed using a microscope-mounted Nikon Coolpix 990 (Nikon GmbH, Düsseldorf, Deutschland) or a Spot camera (Visitron Systems, Puchheim, Germany). Three dimensional models (see below) of the bulb were then reconstructed using the software Amira® 3.0 (TGS Inc., Richmond, USA) on a high performance graphics computer (SGI Onyx2 Infinite Reality; Silicon Graphics Inc., Mountain View, USA). Positions of those glomeruli that possessed innervation by CNTF-ir axons were determined by comparison of the gallocyanin-stained series with a CNTF-immunoreacted series of sections, and marked within the appropriate bulb model. Standard OB mapping depicting innervated glomeruli in a scatter plot of angle versus rostrocaudal distance was carried out using the Glomerular analysis plugin (Version 2.0) for ImageJ available at http://www.uchsc.edu/rmtsc/restrepo/ (Schaefer et al., 2001a).

RESULTS

CNTF-immunoreactivity in rat and mouse olfactory epithelia

In *rats*, CNTF-immunoreactivity was observed in cells with the typical morphology of ONs (Fig. 1). Additionally, light CNTF-immunoreactivity was found in cells lining the excretory ducts of Bowman's glands, especially using ra-CNTFp and a-CNTFm (Fig. 1b). The pattern of immunoreactivity was similar for all antibodies used, irrespective of the tissue prep-

aration or detection methods. In vibratome and cryostat sections of fixed tissue, immunoreaction intensity in ONs was highest using the ra-CNTFp (Fig. 1a–d), very high using the ga-CNTFp (Fig. 1f) and a-CNTFm (Fig. 1e), but considerably lower with high background labeling using cha-CNTFp (Fig. 1j). Double labeling using two different CNTF antibodies (e.g. ra-CNTFp/a-CNTFm or ra-CNTFp/cha-CNTFp; Fig. 1i, j) showed complete colocalization in ONs. The same labeling pattern was found also on paraffin sections of decalcified tissue using ra-CNTFp and a-CNTFm (not shown). In semithin sections of freeze-dried OE, only ra-CNTFp showed intense staining, again with the same pattern as observed in fixed tissue (Fig. 1 g, h).

The number of immunoreactive ONs differed interindividually, in OE of some rats there were only few CNTF-ir neurons scattered at great distances to each other, while in OE of others the number was considerable (e.g. Fig. 1a). In the whole mount preparations, labeled ONs appeared scattered throughout all regions of the OE (not shown). A preponderance of the localization of CNTF-ir ONs in a specific zone corresponding to zones of receptor or adhesion protein expression described previously (Vassar et al., 1993; Strotmann et al., 1994; Yoshihara et al., 1997; Vassalli et al., 2002) was not recognized.

Immunoreaction product filled the ON cell bodies, dendrites, and often olfactory cilia (Fig. 1c). CNTF-immunolabeling was also detected in the nucleus (Fig. 1 g, h). Immunolabeled axons could be followed running toward the basal lamina (Fig. 1d), joining the fila olfactoria in the lamina propria (Fig. 1b), which displayed strong immunoreactivity due to intensely labeled ensheathing cells.

In *wildtype mice*, a-CNTFm gave low signal, immunolabeling intensity using the polyclonal antisera was lower than described for the rat OE with best results using ra-CNTFp. As in rats, CNTF-ir ONs were found throughout the OE. They were often situated in the superficial region of the ON layer (Fig. 2a). Immunoreactivity was intense in cell bodies and dendrites. Immunolabeling in cilia and axons was less strong than in rats, but immunolabeled axons could be recognized in the fila olfactoria (not shown). The frequency of CNTF-ir ONs in all mouse epithelia was much lower than in any of the rat epithelia.

In *CNTF−/−* and *CNTF-lacZ knockin mice*, the general morphology of the epithelium and OB was not altered. Labeled ONs were absent in control immunoreactions and in CNTF −/− mice. However, light labeling of ON dendrites and the occurrence of small (< 0.5 μm) intraepithelial immunoreactive puncta were occasionally observed in both CNTF+/+ and CNTF−/− mice and was therefore considered unspecific (see below).

In OE of *homozygous CNTF-lacZ knockin mice*, immunolabeling and histochemistry for the reporter protein β-ga-

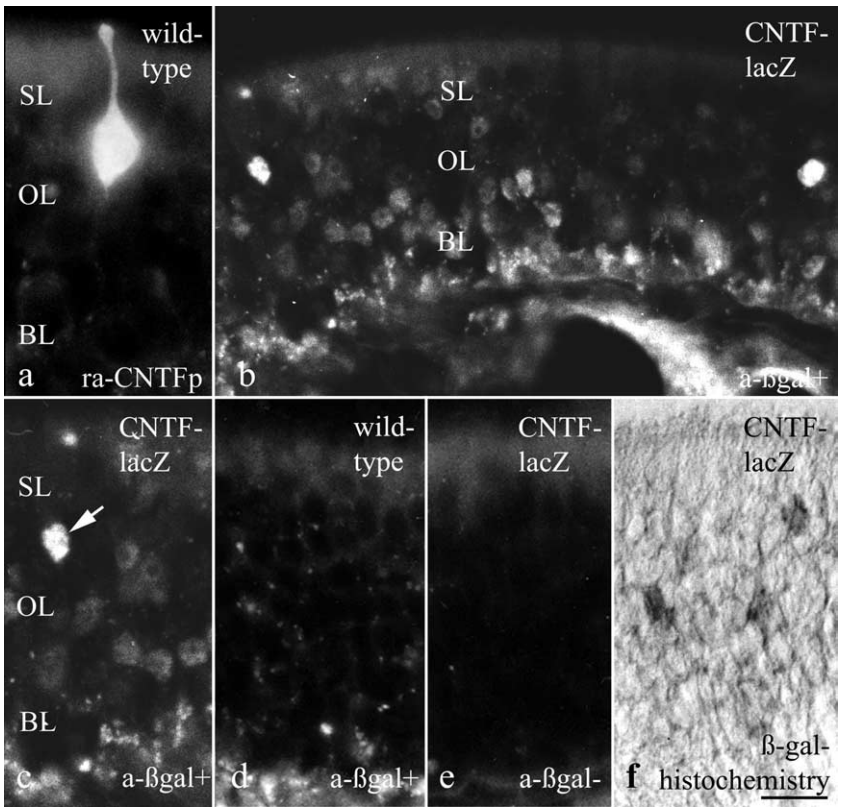

Fig. 2. (a) CNTF-ir ON in wildtype mouse OE (b). An overview over β-galactosidase (β-gal)-immunoreacted OE from a homozygous CNTF-lacZ knockin mouse (CNTF-lacZ) shows nuclei displaying varying intensities of β-gal-immunoreactivity in the OL and BL. (c) Higher magnification demonstrates the localization of a strongly β-gal-ir nucleus in the superficial OL (arrow). (d) In wildtype mice, β-galactosidase-immunolabeling is negative. (e) Omission of primary β-gal-antiserum in CNTF-lacZ knockin mice also shows no labeling. (f) Histochemical staining for β-gal in a homozygous CNTF-lacZ knockin mouse confirms localization of the reporter protein in OL nuclei. Abbreviations see legend to Fig. 1. Scale bar=20 μm in d for a–d.

lactosidase revealed occasionally strong staining of individual nuclei in the superficial olfactory sensory neuron layer (OL; Fig. 2b, f). Additionally, immunolabeling of varying intensity in nuclei in the deeper OL and basal cell layer (BL) was observed (Fig. 2b, c). In heterozygous animals, β-galactosidase-immunoreactivity was found in comparatively fewer nuclei (not shown). Wildtype mice did not show any staining for β-galactosidase (Fig. 2d). Staining was also absent when the β-galactosidase-antiserum was omitted from the incubation (Fig. 2e), or when CNTF wildtype mice were reacted for β-galactosidase histochemistry (not shown).

Characterization of the maturation stage of ONs displaying CNTF-immunoreactivity

Colocalization studies showed that in rats all CNTF-ir ONs were lightly immunoreactive for OMP, a marker for mature neurons (Fig. 3a–c), while colocalization with GAP43, a marker for immature ONs (Mackay-Sim and Chuah, 2000), was never observed (Fig. 3d–f). In DAPI counterstains, the nuclear morphology of the majority of CNTF-ir ONs was normal (Fig. 3 g–i). Only occasionally the chromatin density appeared higher than normal (cf. Fig. 5i–m). CNTF-ir ONs in mice showed the same characteristics (not shown).

Electron microscopically, CNTF-ir terminal axons in rats formed asymmetric synapses with dendrites which received asymmetric and symmetric synapses from other terminals and dendrodendritic synapses (Fig. 4a–c). The immunoreaction product was distributed throughout the axonal cytoplasm, occasionally presenting a somewhat granular appearance. Often, a concentration of immunoreaction product was observed near the presynaptic density (Fig. 4b, c).

Investigations into an association of CNTF-immunoreactivity with ON death

In normal OE, a small number of ONs continuously undergoes apoptosis (Mahalik, 1996; Deckner et al., 1997; Weiler and Farbman, 1997; Cowan and Roskams, 2002). Environmental insults lead to presumably mainly necrotic death of different numbers of ONs depending on the injury extent (Verhaagen et al., 1990; Cowan and Roskams, 2002). We carried out experiments to investigate whether CNTF-immunoreactivity could be linked to imminent ON death.

For apoptosis detection, TUNEL labeling and immunolabeling for CASP were combined with CNTF-immunodetections in rat OE (Deckner et al., 1997; Denecker et al., 2001; Cowan and Roskams, 2002; Kristensen et al., 2003). Additionally, CASP/OMP double labelings were performed to assess the proportion of apoptotically dying mature ONs. The number of TUNEL-labeled cells detected was always small, and TUNEL-CNTF-double-labeled cells were not found (not shown). CASP-ir cells were also few. Most of them were situated in the basal epithelium and did not display OMP-immunoreactivity (Fig. 5a–d). Very rarely, a lightly OMP-ir ON with somewhat distorted morphology displayed CASP-immunoreactivity (Fig. 5e–h). In all CASP-ir cells the nuclear morphology was drastically altered, with fragmented, condensed and clumped chro-

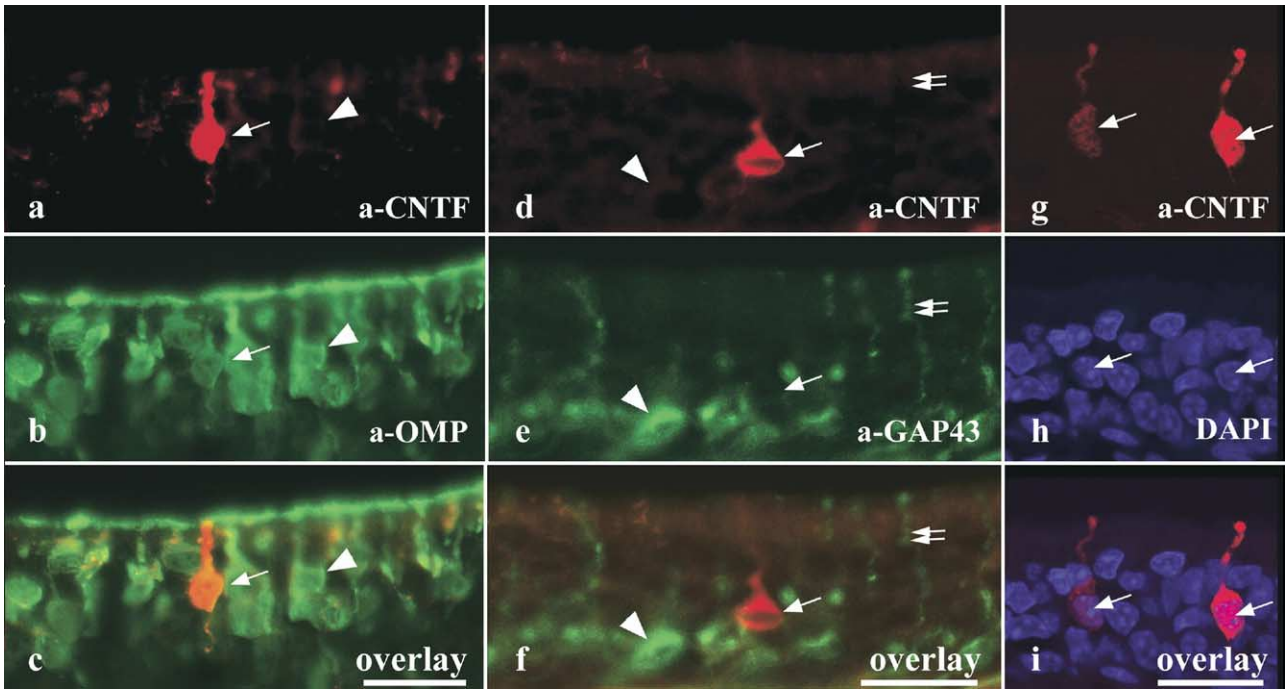

Fig. 3. Confocal images of colocalization studies with OMP- (a–c) and with GAP43-antisera (d–f). CNTF-ir neurons (arrows) are always OMP-, but never GAP43-ir. Arrowheads point to single labeled OMP- or GAP43-ir neurons, double arrows in (d–f) to the dendrite of a GAP43-ir neuron. (g–i) DAPI-counterstaining shows that the nuclear morphology (arrows) of most CNTF-ir neurons is normal. Intranuclear CNTF-immunoreactivity is localized in areas of low chromatin density. Scale bars=20 μm.

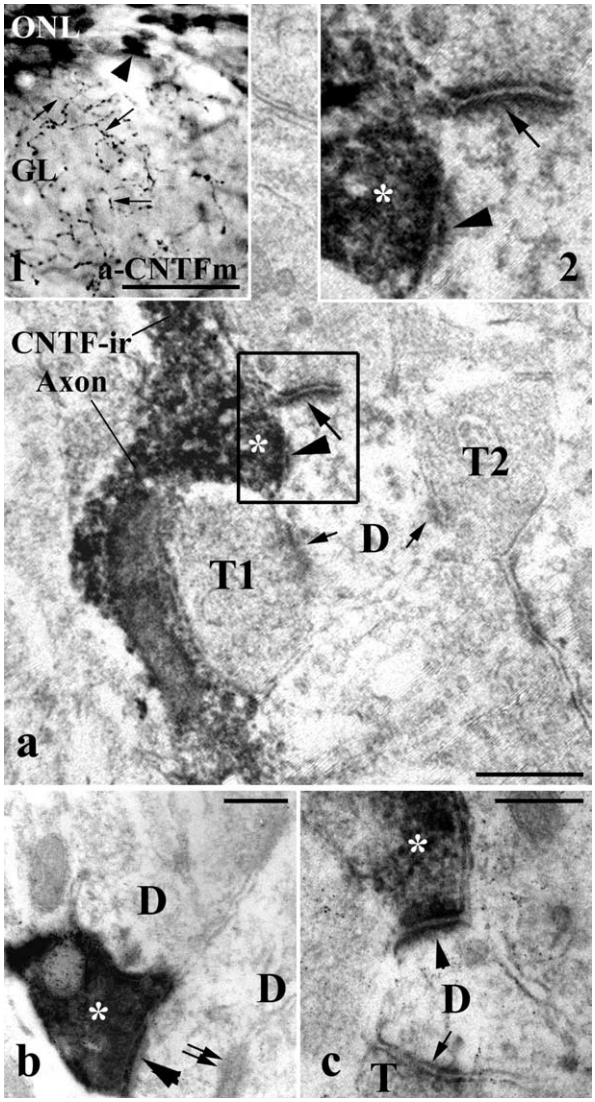

Fig. 4. Electron microscopy (a–c) and light microscopy (inset 1 in a) of CNTF-ir axons in innervated OB glomeruli using a-CNTFm. Inset 1: arrows point to CNTF-ir axons, arrowhead points to a CNTF-ir ensheathing cell of the olfactory nerve layer (ONL). GL, glomerular layer. (a–c) Immunolabeled axonal boutons (asterisks) form asymmetric synapses (arrowheads in a–d, inset 2 in a) with dendrites (D) which are additionally synaptically contacted (arrows) by other, unlabeled terminals (T) and by other D forming reciprocal dendrodendritic contacts (double arrows in b). Scale bar=50 μm in 1, in a–c: 200 nm.

matin (arrows in Fig. 5c/d, g/h, p/q). In colocalization studies for CASP and CNTF, no double-labeled cells were found. Even in the rare CNTF-ir ON displaying condensed nuclear chromatin, CASP-immunoreactivity was absent (Fig. 5i–m).

Chemical lesions of the OE induce ON death within the first few hours post-lesion (Verhaagen et al., 1990; Cowan and Roskams, 2002). Thirty minutes after instillation of a Triton X-100 solution into the right nasal cavity in mice, the morphology of the OE in some regions, especially in the thick parts of the OE lining the nasal roof and upper turbinates was completely normal, while particularly over the septal convexities of the lower turbinates it appeared lightly disturbed in HE-stained sections (not shown). OMP-immunoreactions demonstrated that the cellular and nuclear morphology of the majority of ONs in these areas was normal (double arrows in Fig. 6 b–d), and only few OMP-ir ONs with mildly altered nuclei were found (arrowheads in Fig. 6a–d). Alterations were increased 60 min after lesion (not shown). After 24 h, the epithelium was severely disturbed and occasionally abraded in wide areas of the mucosa, and cellular detritus was observed in the nasal cavity. Only few morphologically normal appearing OMP-ir ONs were left (double arrows in Fig. 6f–h). Mature OMP-ir ONs in different stages of death were recognizable due to their altered morphology and clumped and condensed non-fragmented nuclear chromatin (arrowheads in Fig. 6e–h). OE alterations were very mild to absent in the contralateral nasal cavity or after saline instillation (not shown).

In ra-CNTFp-immunolabeled sections from lesioned CNTF wildtype mice, fluorescence in dendrites appeared increased (small arrows in Fig. 6a, e). In addition to small fluorescent puncta (<0.5 μm in diameter), which were also seen in untreated animals (see above), large intraepithelial fluorescent puncta (>1 μm) were observed in severely altered epithelial areas, which occasionally displayed OMP-immunoreactivity (large arrows in Fig. 6e–h). These puncta were not observed to contain nuclear remnants. Similarly increased fluorescence was also found in CNTF−/− mice in severely disturbed epithelia after lesion, and was therefore considered unspecific, perhaps due to artifactual binding of antibodies to altered tissue constituents (not shown).

In controls and in undisturbed OE 30 min after lesion (as judged from the cellular and nuclear morphology), a few normal-appearing CNTF/OMP double labeled ONs were observed in CNTF wildtype mice, as has been described for untreated mice above. In mildly altered OE 30 min after lesion, the overall CNTF-immunoreactivity was not increased, and ONs with beginning nuclear alterations were not CNTF-ir (arrowheads in Fig. 6a–d). However, CNTF-ir elements displaying light OMP-immunoreactivity and containing condensed remnants of nuclear chromatin were found (large arrows in Fig. 6a–d). Their number was small in all lesioned animals, and similar elements were not observed in comparably well preserved OE in lesioned CNTF−/− mice. In severely disturbed OE 1- or 24 h after lesion, the numerous OMP-ir ONs in different stages of death did not display increased CNTF-immunoreactivity (arrowheads in Fig. 6e-h).

Localization of OB glomeruli containing CNTF-ir ON axons in rats and mice

In our previous study, individual OB glomeruli had been observed to contain plexus of CNTF-ir fibers of different densities (Asan et al., 2003). These CNTF-ir fibers were shown to be immunoreactive for the neural cell adhesion molecule, a marker for all ONs, and for OMP, indicating that they are axons of CNTF-ir mature ONs of the OE. In the present study, parallel CNTF-immunoreacted sections of both OBs in rats and mice were analyzed to assess

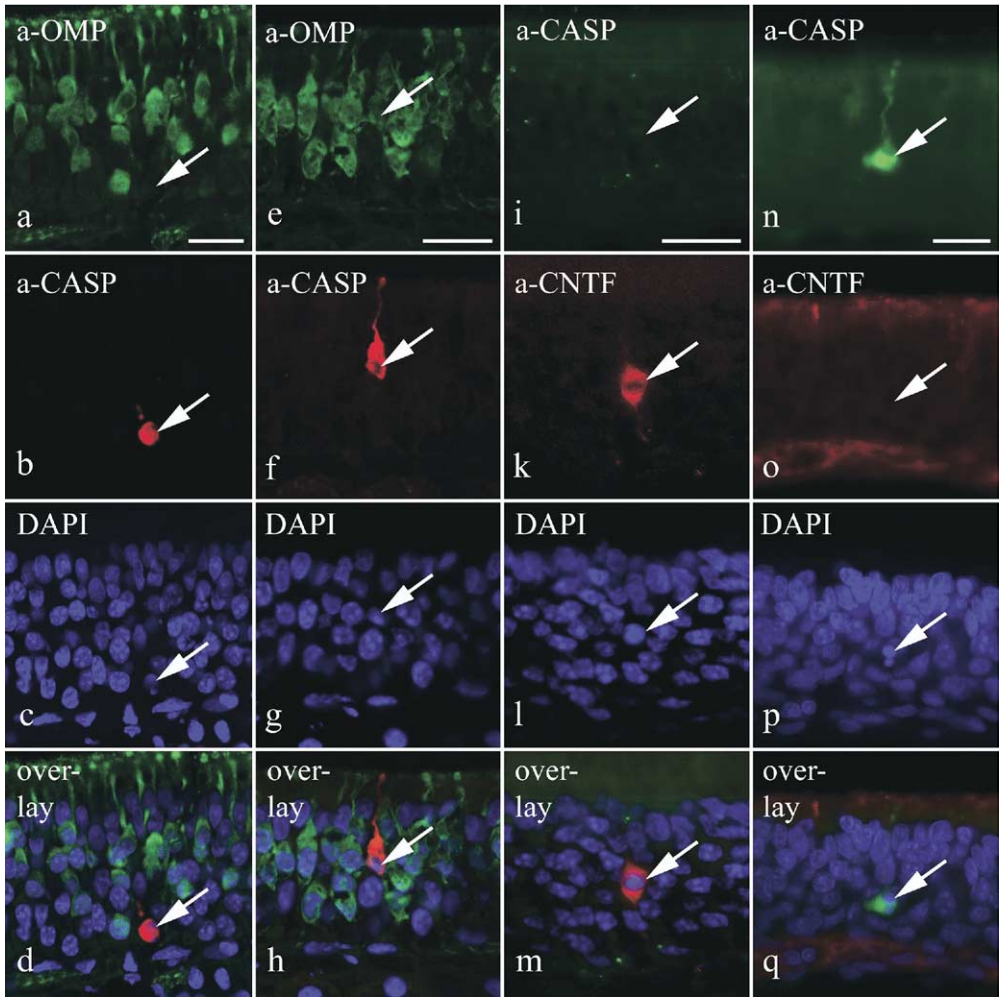

Fig. 5. Confocal images of colocalization studies for OMP and CASP in a–h (OMP: green, CASP: red fluorescence) and for CNTF and CASP in i–q (CNTF: red, CASP: green fluorescence). Most CASP-ir cells are situated in the deep epithelial layers and are not OMP-ir (arrows in a–d). Occasionally, a lightly OMP-ir neuron with distorted morphology displays CASP-immunoreactivity (arrows in e–h). CNTF-ir neurons are not CASP-ir (arrows in i–m), and CASP-ir ONs in the same epithelium as in i–m do not show CNTF-immunoreactivity (arrows in n–q). All CASP-ir neurons contain condensed and fragmented nuclear chromatin (arrows in c/d, g/h, p/q). The nucleus of the CNTF-ir/CASP-negative neuron shown in (k) also shows somewhat condensed but unfragmented chromatin (l). Scale bars=20 μm.

whether CNTF-ir axons were targeted at particular subgroups of glomeruli in both bulbs. In these sections, a strikingly similar localization of many glomeruli containing CNTF-ir fibers was noted in the two bulbs (Fig. 7). To assess the total number and the bilateral positions of glomeruli receiving CNTF-ir axons in individual animals, serial sections of both bulbs from three male (rats 1–3) and three female rats (rats 4–6), and from four female mice were analyzed (Table 1), and three dimensional reconstructions of bulbs and innervated glomeruli were carried out. Additionally, the localization of innervated glomeruli in male rat 1 was recorded in a scatter plot of angle versus rostrocaudal distance depicting cylindrical coordinates of each glomerulus to facilitate comparison of the three dimensional reconstructions with previous glomerular mapping studies (Fig. 8; Schaefer et al., 2001a). Sections were prepared throughout the rostrocaudal lengths of OB pairs (rats: 20 μm sections; mice: 16 μm sections). The sections were collected in six series, so that the first series contained the first, seventh, thirteenth serial section, the second series the second, eighth, fourteenth section, etc. The mean section numbers per series and calculated bulbar lengths for each animal are shown in Table 1. The first series was gallocyanin-stained for cytoarchitectonic analysis, the second was immunoreacted for CNTF. The thickness of the sections was chosen so that glomeruli were present in at least one series analyzed, given glomerular diameters of ~80–160 μm in rats (Shipley, 1995) and ~100 μm in mice (Mombaerts, 2001). For the three dimensional reconstructions, paradigm OBs of each group of animals were chosen, and OB models were constructed from the gallocyanin-stained series of these OBs as described in Experimental Procedures. All sections in the CNTF-immunoreacted series were used for analysis. Detailed comparison of all gallyocyanin and CNTF-reacted serial sections ensured that large glomeruli appearing in two subsequent serial sections were counted only once to avoid double counting. Their localization was deduced

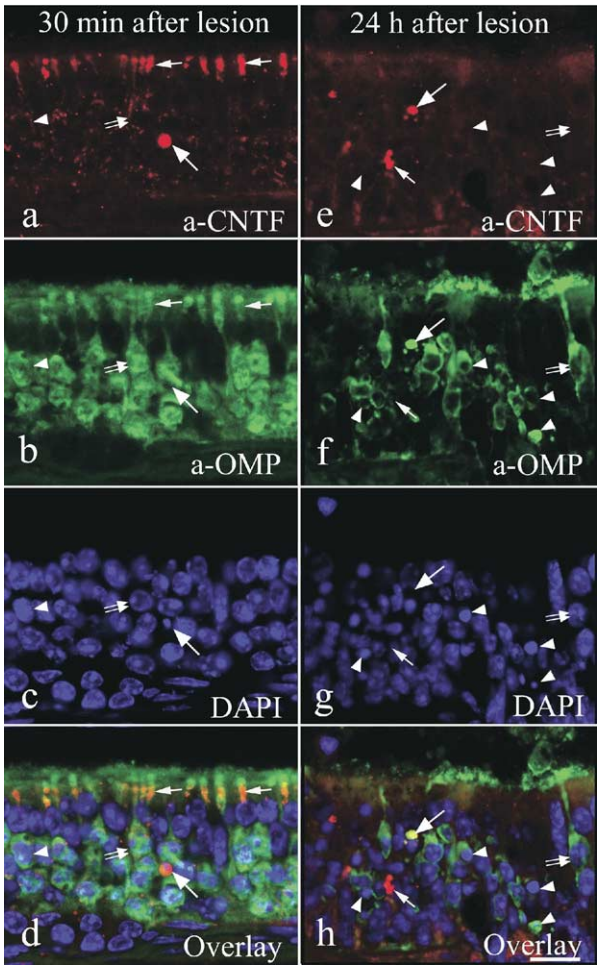

Fig. 6. Confocal images of CNTF/OMP/DAPI labeling of CNTF wild-type mouse OE 30 min (a–d) and 24 h (e–h) after lesion. (a–d) After 30 min, most ONs appear morphologically normal (e.g. double arrows). Only few OMP-ir ONs with beginning nuclear alterations are found (arrowheads). Occasionally, individual CNTF/lightly OMP-ir elements containing condensed nuclei are observed in these mildly altered OE areas (large arrows). Dendritic fluorescence (small arrows) and small (<0.5 μm in diameter) intraepithelial fluorescent puncta after CNTF-immunolabeling are most likely unspecific (details see text). (e–h) Twenty-four hours after lesion, large stretches of the OE are severely disturbed in their morphology. Only few comparatively normal appearing OMP-ir ONs are observed (double arrows). Most OMP-ir ONs display severely altered morphology and contain condensed unfragmented nuclear chromatin (arrowheads). CNTF-immunoreactivity is not increased in these dying ONs. Arrows point to presumably unspecifically labeled, large (>1 μm in diameter) red fluorescent puncta, sometimes colocalizing strong OMP-immunoreactivity (larger arrows) but lacking nuclear remnants (see text). Scale bar=10 μm in h for a–h.

from comparison of the CNTF-immunoreacted series with the gallocyanin-stained series of sections from each animal and marked at the appropriate position into the respective model (Figs. 9 , 10; Supplementary movies 1–6).

In accordance with the lower number of CNTF-ir ONs in the OE, the numbers of glomeruli containing CNTF-ir axons were much lower in OBs of mice than in those of rats. Most of these glomeruli were situated in the ventromedial aspect of the caudal OBs (Fig. 9). The bilateral positions of these glomeruli appeared to be highly similar in two of the four analyzed animals.

In all rat OBs, the numbers of glomeruli targeted by CNTF-ir axons were bilaterally similar but varied interindividually, with some animals displaying more than triple the number of innervated glomeruli in the OBs of both sides than others (Table 1; Fig. 10; Movies 1–5). Innervated glomeruli in all rats were particularly frequent in the ventral, ventrolateral and ventromedial part of the OBs, less were found dorsally and dorsolaterally, and only few in dorsomedial aspects (Figs. 8, 10). In all rats analyzed, comparisons between left and right OBs indicated that for many of the glomeruli innervated by CNTF-ir axons in one OB, glomeruli containing CNTF-ir fibers were found within only few (0–3) glomerular diameters of the exact symmetrical position in the contralateral OB (Fig. 7). Glomeruli in bilaterally similar positions usually additionally possessed CNTF-ir axonal plexus of very similar densities (Fig. 7, insets). It appeared that the relative frequency of positional similarity was higher in OBs with higher numbers of glomeruli innervated by CNTF-ir axons than in those with comparatively low numbers. Systematic differences between male and female rats in the numbers, the predominant localization, or the apparent bilaterally similar positioning of innervated glomeruli were not noted.

DISCUSSION

Early investigations into the localization of CNTF in the rodent olfactory system indicated that in the OB, the specific glial cells of the olfactory nerve layer, the ensheathing cells, produce and contain the protein (Stöckli et al., 1991; Dobrea et al., 1992). This was confirmed in our recent study (Asan et al., 2003), which additionally suggested the presence of CNTF-immunoreactivity in individual ON axons innervating some olfactory glomeruli. Presence of CNTF-immunoreactivity in ONs had previously been suggested by Buckland and Cunningham (1999), who detected CNTF in all cells of the ON lineage in the rat OE and in various neuronal cell types in the OB, while staining in the ensheathing cells or in olfactory axons was not reported. This disagreement with our own findings in the OB prompted us to look again into CNTF localization in the OE. To provide conclusive validation of our CNTF immunodetections, we used four different antibodies under various tissue pretreatment conditions and performed numerous controls including immunolabeling of tissue from CNTF−/− mice. Additionally, we determined the localization of β-galactosidase in mice expressing the reporter gene under the CNTF promoter.

CNTF-immunoreactivity is localized in a small subpopulation of ONs

Using these methods, we documented that individual ONs in rats and mice were intensely CNTF-ir. The number of CNTF-ir ONs differed interindividually in rats. In mice, the number of CNTF-ir ONs was generally lower than in rats. This corresponded to our previous (Asan et al., 2003) and present findings that in rats varying numbers of olfactory

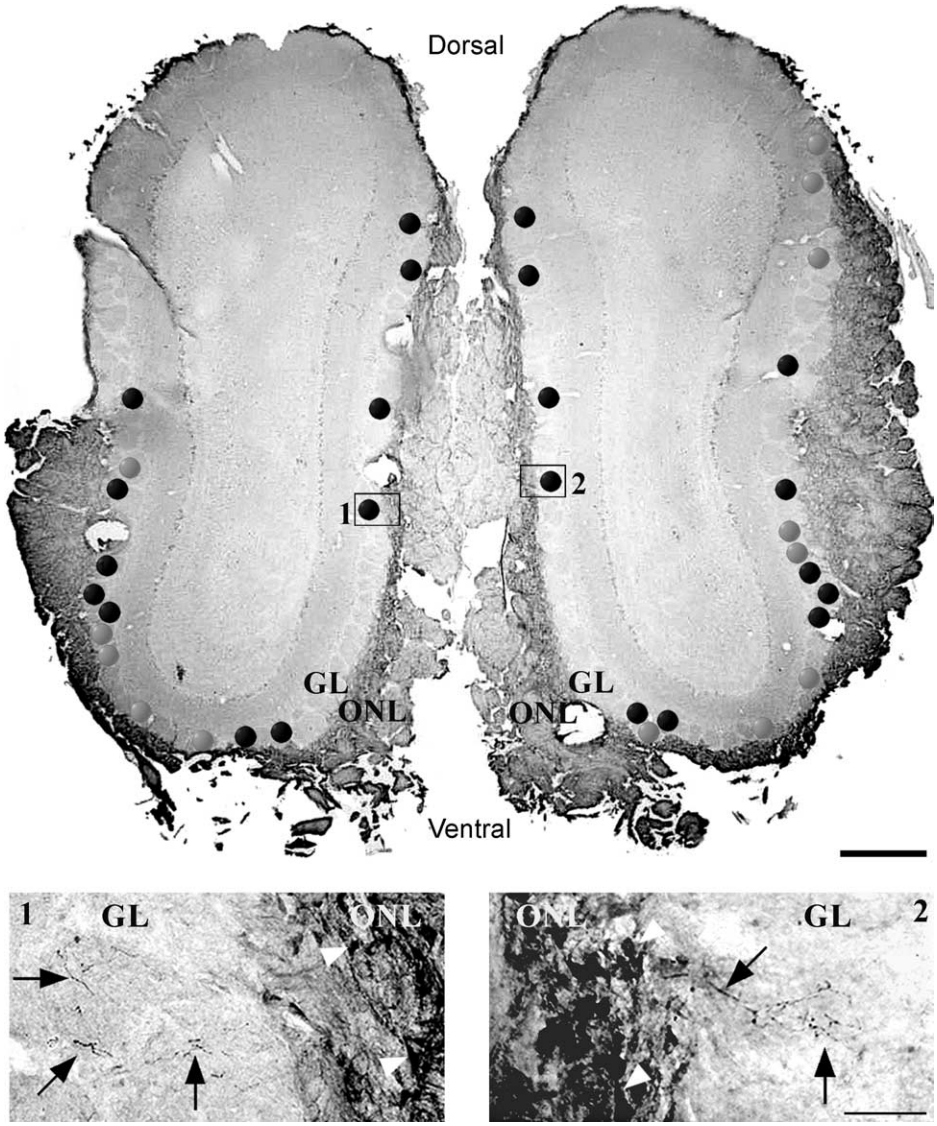

Fig. 7. Frontal ra-CNTFp-reacted sections through the midrostrocaudal level of both OBs of an individual rat. Insets 1 and 2 are magnified images of the two areas boxed in the overview. Immunolabeling of ensheathing cells is obvious in the olfactory nerve layer (ONL; arrowheads in insets 1 and 2). Glomeruli in the glomerular layer (GL) containing CNTF-ir axons are marked by gray and black balls. Black balls exemplify glomeruli innervated by CNTF-ir axons localized in bilaterally similar positions, within not more than three glomerular diameters of exact symmetry. Higher magnification in insets 1 and 2 demonstrates that such symmetrically localized innervated glomeri usually possess similar innervation characteristics, in this case innervation by only few CNTF-ir axons (arrows). Scale bars=500 μm (overview), 50 μm (insets).

glomeruli were innervated by CNTF-ir ON axons, while in mice only few glomeruli received CNTF-ir axons. A general immunoreactivity of cells of the rat ON lineage, as suggested by Buckland and Cunningham (1999), could not be confirmed in our material. Nevertheless, ONs are the first neurons in which CNTF-immunoreactivity has been documented. The finding that typical ON nuclei are β-galactosidase-ir in CNTF-lacZ knockin mice indicates that ONs may indeed express transcripts under the CNTF promoter. Moreover, in another transgenic mouse line with CNTF-promoter-driven β-galactosidase expression, specifically strong transcription of the transgene was found in individual ONs and their axons (Stefanuto et al., 1995). An explanation for the finding that more ONs appear to express the reporter gene in homozygote CNTF-lacZ knockin mice than CNTF-ir ONs are found in CNTF wildtype mice is not readily at hand. However, it has to be borne in mind that the CNTF-lacZ knockin-mice are CNTF-knockouts, which may lead to somewhat altered CNTF-promoter-driven expression in these animals. This suggestion is supported by the finding that, in heterozygous animals, there are less β-gal-reactive ON nuclei found than in homozygous knockin mice.

The additional experiments carried out in the present study were designed to characterize specific properties of CNTF-ir ONs in order to provide a basis for further investigations into possible roles of the factor in this unusual neuronal localization. In principle, two different scenarios

Table 1. Results of analyses carried out on series of sections of both OBs in rats and mice

Animals	Number of sections per series	Specimen length	Numbers of glomeruli innervated by CNTF-ir axons		
			Left OB	Right OB	Total
Male rats (movie 1)					
Rat 1 (Fig. 10a)	53	6360 μm	68	61	129
Rat 2 (movie 2)	60	7200 μm	55	55	110
Rat 3 (movie 3)	53	6360 μm	161	177	338
Mean	55.3	6640 μm			
SEM	±2.33	±280 μm			
Female rats (movie 4)					
Rat 4 (Fig. 10b)	50	6000 μm	36	40	76
Rat 5 (movie 5)	51	6120 μm	134	158	292
Rat 6 (Fig. 10c)	45	5400 μm	146	158	304
Mean	48.7	5840 μm			
SEM	±1.86	±223 μm			
Mice (Fig. 9; movie 6)					
Mouse 1	39	3744 μm	0	4	4
Mouse 2	46	4416 μm	4	6	10
Mouse 3	44	4224 μm	8	4	12
Mouse 4	38	3648 μm	4	3	7
Mean	41.75	4008 μm			
SEM	±1.931	±185.4 μm			

SEM, standard error of the mean. Details see text. Movies of the three dimensional reconstructions are provided as supplementary material.

are at hand, which may account for the occurrence of CNTF-immunoreactivity in a small subpopulation of ONs: 1) CNTF-immunoreactivity could be associated with comparatively short phases of the life cycle of all ONs, or 2) CNTF-immunoreactivity could be restricted to a particular subpopulation of ONs, characterized for instance by the expression and/or activation of specific ORs. We decided to investigate both possibilities in parallel.

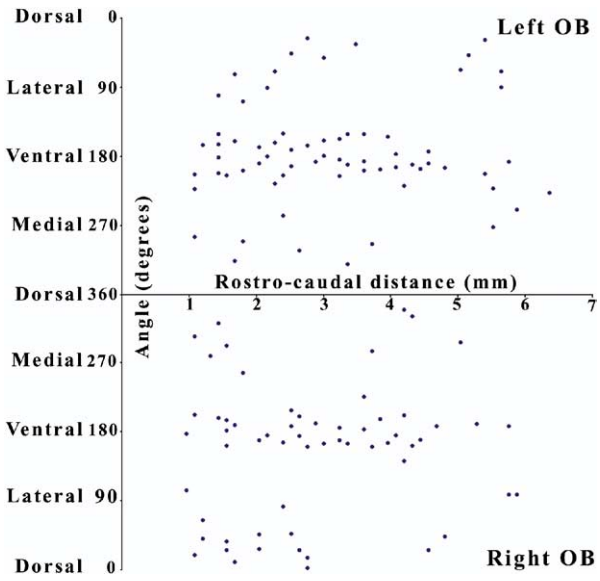

Fig. 8. Two dimensional scatter plot constructed according to Schaefer et al. (2001a), depicting angle around the section and rostrocaudal position of glomeruli innervated by CNTF-ir axons in male rat 1 (cf. Table 1, Fig. 10a), illustrating positions of these glomeruli in left and right bulb in a standard format.

Studies on CNTF-immunoreactivity in specific ON life phases

CNTF-ir ONs detected in the present study displayed morphological criteria for mature sensory neurons involved in olfactory information processing (Schwob et al., 1992): they possessed olfactory vesicles and cilia, and CNTF-ir axons formed typical asymmetric synaptic contacts in the olfactory glomeruli. In addition, CNTF-ir neurons were characterized as mature neurons by their immunoreactivity for OMP, and by the lack of GAP43-immunroeactivity, a marker for immature ONs (e.g. Mackay-Sim and Chuah, 2000; Asan and Drenckhahn, 2005). The CNTF-immunoreaction product filled the ONs completely, from cilia to axon terminals, including chromatin-free areas of the nucleus.

Recently, a nuclear localization of CNTF was demonstrated in rat cortical astrocytes (Bajetto et al., 1999, 2000), and we have detected nuclear CNTF immunoreactivity also in ensheathing cells (Asan et al., 2003). It was suggested that a mechanism of facilitated transport was responsible for the nuclear translocation of the factor, indicating functional relevance of the translocation. Nuclear accumulation of basic fibroblast growth factor 2 and of its receptor has been implicated in the regulation of activation and hypertrophy of human glial cells (Moffett et al., 1998). It will be interesting to investigate whether “intracrine” effects are a function of nuclear CNTF in ONs (see above).

An intriguing observation was made in the electron microscopic study of CNTF-ir axon terminals in the OB: often, there was an accumulation of immunoreaction product found presynaptically. Although the manner of release of CNTF, which lacks a hydrophobic signal peptide for conventional secretion pathways, is still not known, uncon-

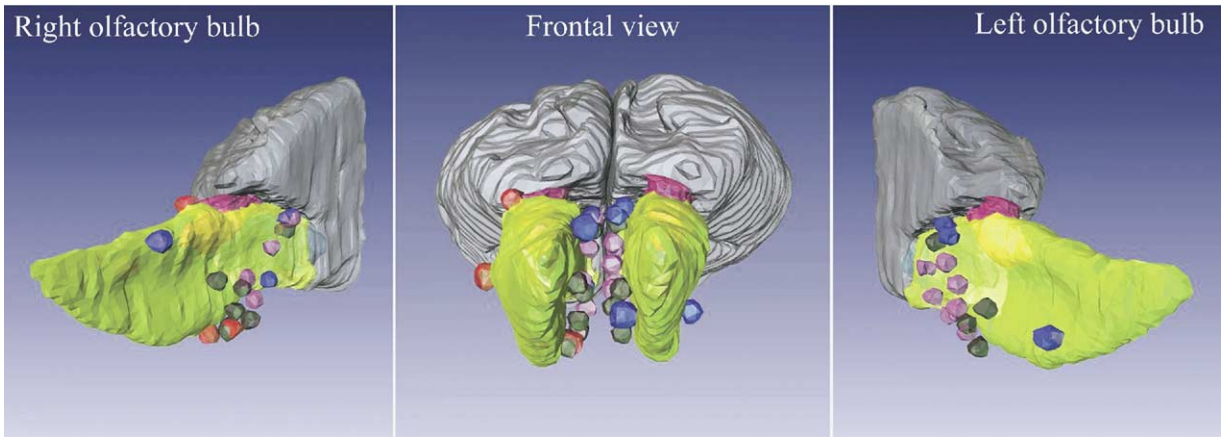

Fig. 9. Three dimensional model of OBs in mice. Gray: frontal cortex. Yellow: main OB mitral cell layer. Mauve: accessory OB mitral cell layer. Red, blue, light mauve and black balls, respectively, indicate the localization of glomeruli with CNTF-ir axons in four mice. For better documentation the size of the balls has been increased to approximately triple the size of the innervated glomeruli. Note that innervated glomeruli are particularly frequent in the posterior ventromedial bulb.

ventional release of such proteins is highly likely (MacKenzie et al., 2001), particularly in cell regions with substantial membrane turnover. Mitral cells express high levels of the high-affinity receptor for CNTF, CNTF receptor alpha (MacLennan et al., 1996; Lee et al., 1997b). It is tempting to speculate that CNTF released at the olfactory axon-mitral cell synapse could be involved in specific mechanisms of olfactory information processing, e.g. synaptic plasticity.

Previous investigations have shown that ONs undergo a constant turnover. ON death occurs due to apoptosis, or, in the case of environmental insults, to necrosis (e.g. Schwob, 2002; Cowan and Roskams, 2002). Mature ONs may live long (up to 12 months and more at least in mice) unless injured, and proliferation in the OE shows an age-related decrease (Hinds et al., 1984; Weiler and Farbman, 1997). Thus, dying ONs are relatively few in number, particularly in mice reared under essentially germ-free conditions. Their number may be increased in animals housed under normal conditions, like the rats used in the present study. Considering the function of CNTF as a lesion factor in other CNS areas, and the differences in CNTF-ir ON numbers between the species, it appeared feasible that CNTF-immunoreactivity could mark a phase of imminent apoptotic and/or necrotic death, when neuronal morphology is still rather well preserved and synaptic contacts are intact yet.

We detected only very few apoptotically dying mature (OMP-ir) ONs in normal rat OE, a finding in accordance with previous investigations (Schwob et al., 1992; Mahalik, 1996). The lack of colocalization of CNTF with apoptosis markers even in CNTF-ir ONs with slightly altered nuclear morphology indicated that CNTF-immunoreactivity did not characterize apoptotically dying OMP-ir ONs.

Light chemical lesions of the OE were carried out to analyze whether exogenous induction of ON death was associated with CNTF-immunoreactivity. Mice were chosen for these experiments for two reasons: firstly, the number of CNTF-ir ONs we detected in this species was always very low and did not vary under normal conditions as extensively as in rats; secondly, reliable specificity controls for the immunoreactions after lesions could be carried out by performing appropriate experiments in CNTF−/− mice. The postlesional morphological alterations of the OE were in accordance with data from the literature (Verhaagen et al., 1990). Numerous OMP-ir ONs displaying characteristics of various stages of degeneration were observed after lesions. A general increase in specific CNTF-immunoreactivity in these dying ONs was not noted. The increase in unspecific fluorescence after CNTF-immunolabeling, which was found in severely damaged OE of CNTF wildtype and knockout mice, again points out the necessity for strict immunolabeling specificity controls under all circumstances. A feature that was observed in CNTF+/+ mice only, and therefore may be specific, was that in areas with very mild alterations only ONs that displayed CNTF-immunoreactivity were found to be damaged. Our findings indicate that CNTF-immunoreactivity is not generally associated with exogenously induced ON death, at least in this model lesion. However, it appears possible that CNTF-ir ONs are more susceptible to toxic insults than non-ir ONs. An increase of CNTF-immunoreactivity in not fatally injured neurons after less drastic insults or at different time points than studied in this investigation cannot be unequivocally excluded.

The localization of glomeruli innervated by CNTF-ir ON axons indicates association of CNTF-immunoreactivity with sensory properties of ONs

Experimental analyses of the olfactory information processing in mice have shown that the population of ONs falls into subpopulations, each expressing only one of a large family of, in mice, about 1000 different ORs. The relatively small subpopulation of ONs expressing the same OR, and thus displaying identical sensory responsiveness to specific odorants, targets one or a few specific olfactory glomeruli in the ipsilateral OB. The “odor map” generated

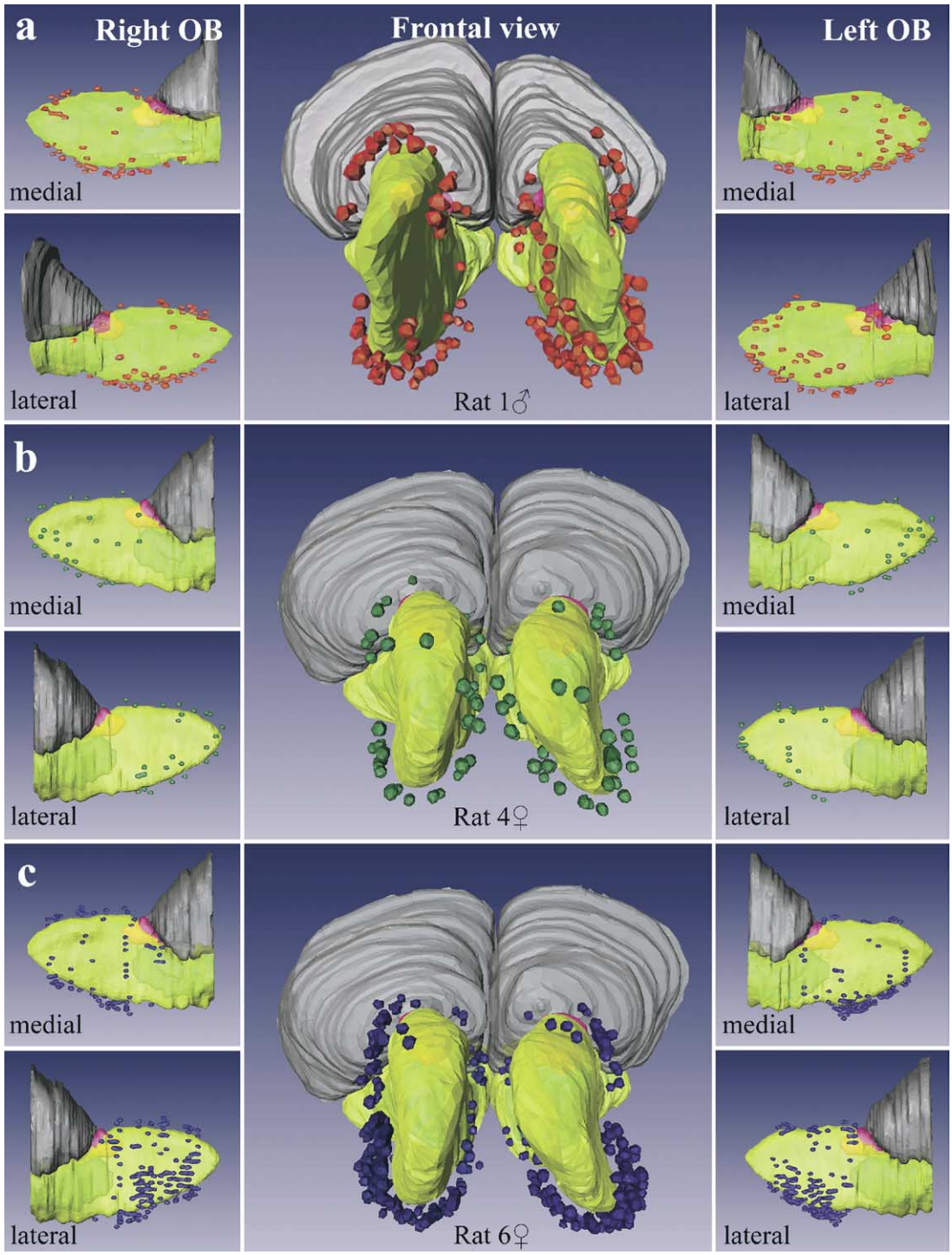

Fig. 10. Three dimensional models of OBs with glomeruli containing CNTF-ir axons in three individual rats (male rat 1, female rats 4 and 6 in Table 1: a, b, c, respectively). Color coding as in Fig. 9. Additionally, the anterior olfactory nucleus is indicated in turquoise. Red, green, and blue balls represent the glomeruli innervated by CNTF-ir fibers in the three animals in a,b,c. Note that these glomeruli are particularly frequently localized in all animals in the ventral mid- to posterior bulbs, and that the number of glomeruli is low in the first female rat (b; rat four in Table 1) but much higher in the first male and third female rat (a,c; rats 1 and 6 in Table 1).

by this wiring is, with small permutations, bilaterally symmetric and interindividually reproducible (Mombaerts et al., 1996; Mombaerts, 1996; Strotmann et al., 2000; Schaefer et al., 2001a; Leon and Johnson, 2003). We found a striking intraindividual bilateral similarity of the positions of glomeruli innervated by CNTF-ir axons, and similar localization patterns of these glomeruli between different animals both in rats and in mice. This result strongly suggests

that CNTF-immunoreactivity characterizes ONs which express the same type of OR, and/or are activated by the same odorants. The fact that the number of glomeruli innervated by CNTF-ir ONs is higher than that found to date for the number of glomeruli innervated by ONs bearing one specific OR (e.g. one to three in mice) indicates that CNTF-ir ONs represent multiple subsets of neurons, which detect more than one odotope, most probably an odorant mixture. It has been shown that odorant mixtures activate ONs situated in different OE areas, leading to spatially defined, bilaterally symmetric glomerular activation patterns, representing odor maps specific for the particular odorant mixtures (Schaefer et al., 2002; Leon and Johnson, 2003).

Glomeruli innervated by CNTF-ir axons are localized preferentially in the ventral and caudomedial part of the OB in mice, and in the ventral, ventrolateral and ventromedial mid- to caudal OB in rats. This localization pattern is similar to the glomerular activation pattern induced by urine odors in mice (Schaefer et al., 2001b, 2002). Urine contains body odors that convey conspecific information about gender, individual identity, reproduction status, and health of the urine donor animal. Schaefer et al. (2001b, 2002) documented that urine odor maps are extremely distinct, reproducible and characteristic for the individual urine donor. The localization of glomeruli activated by specific odorants is similar in rats and mice (Johnson et al., 1999; Inaki et al., 2002; Xu et al., 2003). Thus, it appears possible that, in the present study, CNTF-immunoreactivity characterized ONs sensing urine components in both species.

Interestingly, in a recent study documenting the localization of β-galactosidase expressed under the neurotrophin 3 (NT-3)-promoter in mice during development and postnatally, the reporter protein was found in numerous ONs and in glomeruli situated within the region of the OB activated by urine odors (Vigers et al., 2003). Although the neurotrophic factor itself has not been localized yet, the latter findings together with our results could be interpreted to show that neurotrophic factors may play a particular role in those ONs that subserve the biologically significant conspecific urine odor recognition system (Vigers et al., 2003).

However, the large interindividual differences in the numbers of CNTF-ir ONs and of innervated glomeruli observed particularly in rats would not be expected to occur if the CNTF-immunoreactivity was associated with expression of specific (e.g. urine-sensing) ORs as such. An alternative possibility would be that CNTF-immunoreactivity is associated with intense and/or permanent stimulation of ONs. Under the animal housing conditions employed in our study, urine odors are likely to be prevalent and permanent odors to which the animals are exposed. Differences in urine odor concentration levels and/or sniffing activity may well have occurred between our experimental animals, causing the observed interindividual variations. The hypothesis that CNTF-immunoreactivity is related to sensory activity would not only explain the glomerular innervation patterns observed. It also offers interpretations for CNTF functions based on our morphological findings in ONs. Thus, CNTF in activated neurons could play a role in olfactory neuroplasticity following odorant exposure, for instance by influencing mitral cell plasticity upon being released from ON axon terminals (see above). In addition, or alternatively, CNTF could be an “intracrine” protection factor against overactivation. Experiments testing the different hypotheses are under way.

Other CNTF-ir cell types in the OE

CNTF-ir cells other than ONs were only observed in the rat, and were comparatively lightly immunoreactive. Excretory duct cells of Bowman’s glands almost regularly displayed CNTF-immunoreactivity. Excretory duct cells are specialized cells which may contribute to the mucus composition (Okamura et al., 1999; Ferrari et al., 2000). They have also been suggested to represent progenitor cells for non-neuronal cell types in the OE, and thus represent a glial-precursor like cell type (Huard et al., 1998). The olfactory mucus contains dopamine (Lucero and Squires, 1998), IGF-I (Federico et al., 1999), and possibly also GDNF (Mackay-Sim and Chuah, 2000). Factors in the mucus may influence differentiation and survival of ONs that have reached the luminal surface (Mackay-Sim and Chuah, 2000), and if CNTF were secreted by excretory duct cells, it could also play a role in these processes.

Acknowledgments—The authors are indebted to Rita Herrmann, Sieglinde Schenk and Karin Reinfurth for expert technical assistance, and to Drs. F. Margolis and H.-D. Hofmann for generous gifts of antibodies. The study was supported by the Deutsche Forschungsgemeinschaft, SFB 581, TP Z3 and B4.

APPENDIX
SUPPLEMENTARY DATA

Supplementary data associated with this article can be found, in the online version, at doi: 10.1016/j.neuroscience.2005.05.017.

REFERENCES

Asan E, Drenckhahn D (2005) Immunocytochemical characterization of two types of microvillar cells in rodent olfactory epithelium. Histochem Cell Biol 123:157–168.

Asan E, Langenhan T, Holtmann B, Bock H, Sendtner M, Carroll P (2003) Ciliary neurotrophic factor in the olfactory bulb of rats and mice. Neuroscience 120:99–112.

Asan E, Meier-Stiegen S (1998) Localization of proteins associated with the junctional complex in the rat olfactory epithelium. Eur J Neurosci 10 (Suppl 10):360–365.

Bajetto A, Barbero S, Bonavia R, Chimini G, Schettini G (2000) Immunofluorescence and biochemical techniques to detect nuclear localization of ciliary neurotrophic factor in glial cells. Brain Res Brain Res Protoc 5:273–281.

Bajetto A, Schettini G, Chimini G (1999) Nuclear localization of ciliary neurotrophic factor in glial cells. Brain Res 818:565–569.

Barnett SC, Alexander CL, Iwashita Y, Gilson JM, Crowther J, Clark L, Dunn LT, Papanastassiou V, Kennedy PG, Franklin RJ (2000) Identification of a human olfactory ensheathing cell that can effect transplant-mediated remyelination of demyelinated CNS axons. Brain 123 (Pt 8):1581–1588.

Bartolomei JC, Greer CA (2000) Olfactory ensheathing cells: bridging the gap in spinal cord injury. Neurosurgery 47:1057–1069.

Berod A, Hartman BK, Pujol JF (1981) Importance of fixation in immunohistochemistry: use of formaldehyde solutions at variable pH for the localization of tyrosine hydroxylase. J Histochem Cytochem 29:844–850.

Buckland ME, Cunningham AM (1999) Alterations in expression of the neurotrophic factors glial cell line-derived neurotrophic factor, ciliary neurotrophic factor and brain-derived neurotrophic factor, in the target-deprived olfactory neuroepithelium. Neuroscience 90: 333–347.

Cowan CM, Roskams AJ (2002) Apoptosis in the mature and developing olfactory neuroepithelium. Microsc Res Tech 58:204–215.

Dallner C, Woods AG, Deller T, Kirsch M, Hofmann HD (2002) CNTF and CNTF receptor alpha are constitutively expressed by astrocytes in the mouse brain. Glia 37:374–378.

Deckner ML, Risling M, Frisen J (1997) Apoptotic death of olfactory sensory neurons in the adult rat. Exp Neurol 143:132–140.

Denecker G, Vercammen D, Steemans M, Vanden Berghe T, Brouckaert G, Van Loo G, Zhivotovsky B, Fiers W, Grooten J, Declercq W, Vandenabeele P (2001) Death receptor-induced apoptotic and necrotic cell death: differential role of caspases and mitochondria. Cell Death Differ 8:829–840.

Dobrea GM, Unnerstall JR, Rao MS (1992) The expression of CNTF message and immunoreactivity in the central and peripheral nervous system of the rat. Brain Res Dev Brain Res 66:209–219.

Drenckhahn D, Franz H (1986) Identification of actin-, alpha-actinin-, and vinculin-containing plaques at the lateral membrane of epithelial cells. J Cell Biol 102:1843–1852.

Federico G, Maremmani C, Cinquanta L, Baroncelli GI, Fattori B, Saggese G (1999) Mucus of the human olfactory epithelium contains the insulin-like growth factor-I system which is altered in some neurodegenerative diseases. Brain Res 835:306–314.

Ferrari CC, Carmanchahi PD, Aldana Marcos HJ, Affanni JM (2000) Ultrastructural characterisation of the olfactory mucosa of the armadillo Dasypus hybridus (Dasypodidae, Xenarthra). J Anat 196 (Pt 2):269–278.

Gheusi G, Cremer H, McLean H, Chazal G, Vincent JD, Lledo PM (2000) Importance of newly generated neurons in the adult olfactory bulb for odor discrimination. Proc Natl Acad Sci U S A 97:1823–1828.

Giess R, Goetz R, Schrank B, Ochs G, Sendtner M, Toyka K (1998) Potential implications of a ciliary neurotrophic factor gene mutation in a German population of patients with motor neuron disease. Muscle Nerve 21:236–238.

Guthrie KM, Woods AG, Nguyen T, Gall CM (1997) Astroglial ciliary neurotrophic factor mRNA expression is increased in fields of axonal sprouting in deafferented hippocampus. J Comp Neurol 386:137–148.

Heinsen H, Arzberger T, Schmitz C (2000) Celloidin mounting (embedding without infiltration): a new, simple and reliable method for producing serial sections of high thickness through complete human brains and its application to stereological and immunohistochemical investigations. J Chem Neuroanat 20:49–59.

Hinds JW, Hinds PL, McNelly NA (1984) An autoradiographic study of the mouse olfactory epithelium: evidence for long-lived receptors. Anat Rec 210:375–383.

Huard JM, Youngentob SL, Goldstein BJ, Luskin MB, Schwob JE (1998) Adult olfactory epithelium contains multipotent progenitors that give rise to neurons and non-neural cells. J Comp Neurol 400:469–486.

Inaki K, Takahashi YK, Nagayama S, Mori K (2002) Molecular-feature domains with posterodorsal-anteroventral polarity in the symmetrical sensory maps of the mouse olfactory bulb: mapping of odourant-induced Zif268 expression. Eur J Neurosci 15:1563–1574.

Johnson BA, Woo CC, Hingco EE, Pham KL, Leon M (1999) Multidimensional chemotopic responses to n-aliphatic acid odorants in the rat olfactory bulb. J Comp Neurol 409:529–548.

Kalderon D, Roberts BL, Richardson WD, Smith AE (1984) A short amino acid sequence able to specify nuclear location. Cell 39: 499–509.

Kristensen BW, Noer H, Gramsbergen JB, Zimmer J, Noraberg J (2003) Colchicine induces apoptosis in organotypic hippocampal slice cultures. Brain Res 964:264–278.

Kugler P, Wolf G, Scherberich J (1985) Histochemical demonstration of peptidases in the human kidney. Histochemistry 83:337–341.

Lee MY, Deller T, Kirsch M, Frotscher M, Hofmann HD (1997a) Differential regulation of ciliary neurotrophic factor (CNTF) and CNTF receptor alpha expression in astrocytes and neurons of the fascia dentata after entorhinal cortex lesion. J Neurosci 17:1137–1146.

Lee MY, Hofmann HD, Kirsch M (1997b) Expression of ciliary neurotrophic factor receptor-alpha messenger RNA in neonatal and adult rat brain: an in situ hybridization study. Neuroscience 77:233–246.

Leon M, Johnson BA (2003) Olfactory coding in the mammalian olfactory bulb. Brain Res Brain Res Rev 42:23–32.

Linker RA, Maurer M, Gaupp S, Martini R, Holtmann B, Giess R, Rieckmann P, Lassmann H, Toyka KV, Sendtner M, Gold R (2002) CNTF is a major protective factor in demyelinating CNS disease: a neurotrophic cytokine as modulator in neuroinflammation. Nat Med 8:620–624.

Liposits Z, Sherman D, Phelix C, Paull WK (1986) A combined light and electron microscopic immunocytochemical method for the simultaneous localization of multiple tissue antigens. Tyrosine hydroxylase immunoreactive innervation of corticotropin releasing factor synthesizing neurons in the paraventricular nucleus of the rat. Histochemistry 85:95–106.

Lipson AC, Widenfalk J, Lindqvist E, Ebendal T, Olson L (2003) Neurotrophic properties of olfactory ensheathing glia. Exp Neurol 180:167–171.

Lucero MT, Squires A (1998) Catecholamine concentrations in rat nasal mucus are modulated by trigeminal stimulation of the nasal cavity. Brain Res 807:234–236.

Mackay-Sim A, Chuah MI (2000) Neurotrophic factors in the primary olfactory pathway. Prog Neurobiol 62:527–559.

MacKenzie A, Wilson HL, Kiss-Toth E, Dower SK, North RA, Surprenant A (2001) Rapid secretion of interleukin-1beta by microvesicle shedding. Immunity 15:825–835.

MacLennan AJ, Vinson EN, Marks L, McLaurin DL, Pfeifer M, Lee N (1996) Immunohistochemical localization of ciliary neurotrophic factor receptor alpha expression in the rat nervous system. J Neurosci 16:621–630.

Mahalik TJ (1996) Apparent apoptotic cell death in the olfactory epithelium of adult rodents: Death occurs at different developmental stages. J Comp Neurol 372:457–464.

Masu Y, Wolf E, Holtmann B, Sendtner M, Brem G, Thoenen H (1993) Disruption of the CNTF gene results in motor neuron degeneration. Nature 365:27–32.

Matsuoka M, Kaba H, Mori Y, Ichikawa M (1997) Synaptic plasticity in olfactory memory formation in female mice. Neuroreport 8: 2501–2504.

Miragall F, Kadmon G, Husmann M, Schachner M (1988) Expression of cell adhesion molecules in the olfactory system of the adult mouse: presence of the embryonic form of N-CAM. Dev Biol 129: 516–531.

Miwa T, Moriizumi T, Horikawa I, Uramoto N, Ishimaru T, Nishimura T, Furukawa M (2002) Role of nerve growth factor in the olfactory system. Microsc Res Tech 58:197–203.

Moffett J, Kratz E, Myers J, Stachowiak EK, Florkiewicz RZ, Stachowiak MK (1998) Transcriptional regulation of fibroblast growth factor-2 expression in human astrocytes: implications for cell plasticity. Mol Biol Cell 9:2269–2285.

Mombaerts P (1996) Targeting olfaction. Curr Opin Neurobiol 6:481–486.

Mombaerts P (2001) How smell develops. Nat Neurosci 4 (Suppl):1192–1198.

Mombaerts P, Wang F, Dulac C, Chao SK, Nemes A, Mendelsohn M, Edmondson J, Axel R (1996) Visualizing an olfactory sensory map. Cell 87:675–686.

Nagao H, Yamaguchi M, Takahash Y, Mori K (2002) Grouping and representation of odorant receptors in domains of the olfactory bulb sensory map. Microsc Res Tech 58:168–175.

Nibu K (2002) Introduction to olfactory neuroepithelium. Microsc Res Tech 58:133–134.

Oberto M, Soncin I, Bovolin P, Voyron S, De Bortoli M, Dati C, Fasolo A, Perroteau I (2001) ErbB-4 and neuregulin expression in the adult mouse olfactory bulb after peripheral denervation. Eur J Neurosci 14:513–521.

Okamura H, Sugai N, Suzuki K (1999) Localization of carbonic anhydrase in guinea pig Bowman's glands. J Histochem Cytochem 47:1525–1532.

Perez-Bouza A, Wigley CB, Nacimiento W, Noth J, Brook GA (1998) Spontaneous orientation of transplanted olfactory glia influences axonal regeneration. Neuroreport 9:2971–2975.

Raisman G (2000) Repair of corticospinal axons by transplantation of olfactory ensheathing cells. Novartis Found Symp 231:94–97.

Reynolds ES (1963) The use of lead citrate at high pH as an electron opaque stain in electron microscopy. J Cell Biol 17:208–212.

Schaefer ML, Finger TE, Restrepo D (2001a) Variability of position of the P2 glomerulus within a map of the mouse olfactory bulb. J Comp Neurol 436:351–362.

Schaefer ML, Young DA, Restrepo D (2001b) Olfactory fingerprints for major histocompatibility complex-determined body odors. J Neurosci 21:2481–2487.

Schaefer ML, Yamazaki K, Osada K, Restrepo D, Beauchamp GK (2002) Olfactory fingerprints for major histocompatibility complex-determined body odors II: relationship among odor maps, genetics, odor composition, and behavior. J Neurosci 22:9513–9521.

Schwob JE (2002) Neural regeneration and the peripheral olfactory system. Anat Rec 269:33–49.

Schwob JE, Szumowski KE, Stasky AA (1992) Olfactory sensory neurons are trophically dependent on the olfactory bulb for their prolonged survival. J Neurosci 12:3896–3919.

Sendtner M, Carroll P, Holtmann B, Hughes RA, Thoenen H (1994) Ciliary neurotrophic factor. J Neurobiol 25:1436–1453.

Shipley MT (1995) The olfactory system. In: The rat nervous system (Paxinos G, ed), pp 899–926. San Diego: Academic Press.

Smale KA, Doucette R, Kawaja MD (1996) Implantation of olfactory ensheathing cells in the adult rat brain following fimbria-fornix transection. Exp Neurol 137:225–233.

Stefanuto G, Cerrato M, Chiocchetti A, Tolosano E, Hirsch E, Cristofori R, Silengo L, Altruda F (1995) Analysis of regulatory regions of the ciliary neutrophic factor gene in transgenic mice. Neuroreport 7: 57–60.

Stöckli KA, Lillien LE, Naher-Noe M, Breitfeld G, Hughes RA, Raff MC, Thoenen H, Sendtner M (1991) Regional distribution, developmental changes, and cellular localization of CNTF-mRNA and protein in the rat brain. J Cell Biol 115:447–459.

Strotmann J, Conzelmann S, Beck A, Feinstein P, Breer H, Mombaerts P (2000) Local permutations in the glomerular array of the mouse olfactory bulb. J Neurosci 20:6927–6938.

Strotmann J, Wanner I, Helfrich T, Beck A, Meinken C, Kubick S, Breer H (1994) Olfactory neurones expressing distinct odorant receptor subtypes are spatially segregated in the nasal neuroepithelium. Cell Tissue Res 276:429–438.

Takahashi R, Yokoji H, Misawa H, Hayashi M, Hu J, Deguchi T (1994) A null mutation in the human CNTF gene is not causally related to neurological diseases. Nat Genet 7:79–84.

Thome J, Nara K, Foley P, Michel T, Gsell W, Retz W, Rosler M, Riederer P (1997) Ciliary neurotrophic factor (CNTF) genotypes: influence on choline acetyltransferase (ChAT) and acetylcholine esterase (AChE) activities and neurotrophin 3 (NT3) concentration in human post mortem brain tissue. J Hirnforsch 38:443–451.

Tisay KT, Key B (1999) The extracellular matrix modulates olfactory neurite outgrowth on ensheathing cells. J Neurosci 19:9890–9899.

Vassalli A, Rothman A, Feinstein P, Zapotocky M, Mombaerts P (2002) Minigenes impart odorant receptor-specific axon guidance in the olfactory bulb. Neuron 35:681–696.

Vassar R, Ngai J, Axel R (1993) Spatial segregation of odorant receptor expression in the mammalian olfactory epithelium. Cell 74: 309–318.

Verhaagen J, Oestreicher AB, Grillo M, Khew-Goodall YS, Gispen WH, Margolis FL (1990) Neuroplasticity in the olfactory system: differential effects of central and peripheral lesions of the primary olfactory pathway on the expression of B-50/GAP43 and the olfactory marker protein. J Neurosci Res 26:31–44.

Vigers AJ, Bottger B, Baquet ZC, Finger TE, Jones KR (2003) Neurotrophin-3 is expressed in a discrete subset of olfactory receptor neurons in the mouse. J Comp Neurol 463:221–235.

Weiler E, Farbman AI (1997) Proliferation in the rat olfactory epithelium: Age-dependent changes. J Neurosci 17:3610–3622.

Weisenhorn DM, Roback J, Young AN, Wainer BH (1999) Cellular aspects of trophic actions in the nervous system. Int Rev Cytol 189:177–265.

Winter CG, Saotome Y, Levison SW, Hirsh D (1995) A role for ciliary neurotrophic factor as an inducer of reactive gliosis, the glial response to central nervous system injury. Proc Natl Acad Sci U S A 92:5865–5869.

Xu F, Liu N, Kida I, Rothman DL, Hyder F, Shepherd GM (2003) Odor maps of aldehydes and esters revealed by functional MRI in the glomerular layer of the mouse olfactory bulb. Proc Natl Acad Sci U S A 100:11029–11034.

Yoshihara Y, Kawasaki M, Tamada A, Fujita H, Hayashi H, Kagamiyama H, Mori K (1997) OCAM: A new member of the neural cell adhesion molecule family related to zone-to-zone projection of olfactory and vomeronasal axons. J Neurosci 17:5830–5842.

Zaborszky L, Heimer L (1989) Combinations of tracer techniques, especially HRP and PHA-L, with transmitter identification for correlated light and electron microscopic studies. In: Neuroanatomical tract tracing methods 2 (Heimer L, Zaborszky L, eds), pp 49–96. New York: Plenum.

(Accepted 12 May 2005)